Complementary mass spectrometry and bioassays for evaluating pharmaceutical-transformation products in treatment of drinking water and wastewater

Jelena Radjenović, Mira Petrović, Damià Barceló

This article summarizes existing studies on complementary mass spectrometry (MS) and bioassays for evaluating treatment processes for drinking water and wastewater [e.g., chlorination, ozonation and advanced oxidation processes (e.g., TiO_2 photocatalytic oxidation, photo-Fenton)] in eliminating pharmaceutical residues. The toxicities of transformation products of pharmaceuticals were rarely determined individually, so we also cover research papers dealing with the total toxicity of the treated solution. To illustrate possible strategies when performing qualitative analysis, we discuss studies based on the use of conventional MS methods, and advanced MS methods involving multiple MS (MS^n) experiments [i.e. triple quadrupole (QqQ-MS) and ion trap (IT-MS)] and accurate mass measurements [i.e. time-of-flight (ToF-MS) and LTQ Orbitrap-MS].

Keywords: Advanced oxidation process; Bioassay; Chlorination; Degradation product; Drinking-water treatment; Mass spectrometry; Ozonation; Pharmaceutical; Transformation product; Wastewater treatment

Jelena Radjenović, Mira Petrović, Damià Barceló
Department of Environmental Chemistry, IDAEA-CSIC, c/Jordi Girona 18-26, 08034 Barcelona, Spain

Mira Petrović*
Institucio Catalana de Reserca i Estudis Avanzats (ICREA), Barcelona, Spain

Damià Barceló
Institut Català de Recerca de l'Aigua (ICRA), Parc Científic i Tecnológic de la Universitat de Girona, Pic de Peguera, 15, 17003 Girona, Spain

*Corresponding author.
Tel.: +34 934 006 100;
fax: +34 932 145 904x432;
E-mail: mpeqam@cid.csic.es

1. Introduction

In the vast array of contaminants of anthropogenic origin reaching our water supplies, pharmaceuticals are among those most continually input into the environment, especially over-the-counter drugs. Most modern drugs are small organic compounds with molecular weight below 500 Da and are designed to have specific pharmacological and physiological effects at low doses, so they are inherently potent and often have unintended effects in wildlife.

After oral, parenteral and/or topical administration, a pharmaceutical is excreted via liver and/or kidneys as a mixture of parent compound and metabolites that are usually more polar and hydrophilic than the original drug [1]. The extent of drug metabolism in the human body varies greatly, ranging from complete metabolization (e.g., carbamazepine and diazepam) to no metabolization (e.g., iopromide and diatrizoate). The cytochrome P450-mediated phase-I metabolism of drugs can result in more reactive compounds, as a result of introducing a functional group or unmasking one (e.g., hydroxylation, epoxidation, reduction and hydrolysis). Furthermore, many phase-I products undergo subsequent phase-II reaction with an endogenous substrate (e.g., glucuronic acid, sulfuric acid, acetic acid or an amino acid), which leads to the formation of highly polar conjugates that are excreted in the urine or bile.

Such conjugates can be cleaved back by the bacterial enzymes during biological wastewater treatment, releasing the parent molecules, so a large fraction of pharmaceuticals will be discharged into wastewater unchanged or in the form of degradation products that are often hardly eliminable in conventional wastewater-treatment plants (WWTPs) [2]. The

0165-9936/$ - see front matter © 2009 Elsevier Ltd. All rights reserved. doi:10.1016/j.trac.2009.02.006

extensive literature on the occurrence of pharmaceuticals in WWTP effluents reinforces concerns about discharged pharmaceutical residues that may end up in the water supply, potentially resulting in adverse effects for humans and the environment.

Some of these adverse environmental effects of pharmaceuticals are toxicity, development of resistant pathogenic bacteria, genotoxicity and endocrine disruption [3,4]. Although many pharmaceuticals do not exhibit acute toxicity, they can have a significant cumulative effect on the metabolism of non-target organisms [5] and the ecosystem as a whole [6]. Pharmaceutical compounds target specific receptors in humans, whereas many of them are common with other mammals, vertebrates and invertebrates. For example, ß-blockers bind to ß-andregenic receptors in humans and block the action of catecholamines (i.e. noradrenalin and adrenalin). However, their effect was seen on fish [7] and invertebrate *Daphnia magna* [8]. More importantly, even when their toxicity as individual compounds is negligible, they might act in an additive manner in a mixture with other ß-blockers and/or their metabolites exhibiting the same mode of action, as shown in the test with *D. magna* [9] and phototoxicity assays with *Vibrio fischeri* [10]. For diclofenac, harmful effects were reported on rainbow-trout fish [11]. Also, antibiotics present in the environment could lead to selection of resistant bacterial strains [12]. Furthermore, knowledge is greatly lacking on the possibilities of pharmaceutical residues reaching humans through biomagnification in the food chain.

Recent studies demonstrated the capability of some pharmaceuticals (e.g., antidepressants, ß-blockers or lipid regulators) to bioaccumulate in aquatic organisms [9,13]. Also, all of the abovementioned ecotoxicological effects of pharmaceuticals are of even more concern if their concentration levels in the aquatic environment increase (e.g., due to demographic reasons with an increasing percentage of older people, as can be expected in the decades ahead).

In attempts to reduce the discharge of pharmaceutical residues into the environment, chemical-oxidation processes [e.g., ozonation and advanced oxidation processes (AOPs)] have been widely investigated as alternatives for the treatment of secondary wastewater effluent, and in the pre-treatment and disinfection step of drinking water (see Fig. 1 [14]).

Also, behavior and elimination of pharmaceuticals have been studied during chlorination, which is a final step of treatment for drinking water and wastewater to reduce microbial contamination. Chlorination with chlorine dioxide and chlorine usually renders both chlorination and oxidation products, whereas concerns exist that products with increased toxicity and biological activity relative to the parent compound might be generated.

For disinfection and oxidation, ozone (O_3) is another widely used oxidant in drinking water (e.g., for taste and odor control, discoloration, micropollutant elimination). During ozonation, organic compounds either directly react with O_3 in specific reactions, or they decompose through hydroxyl ($^{\bullet}OH$) radical-mediated reactions. Molecular O_3 and $^{\bullet}OH$ radical have high oxidation potentials, 2.07 V and 2.80 V, respectively [15]. While O_3 is highly selective towards nucleophilic moieties (e.g., carbon-carbon double bonds, aromatic rings, sulfur, phosphorus, nitrogen and oxygen atoms), $^{\bullet}OH$ radical is non-selective and can react with various organic and inorganic compounds through hydrogen abstraction, radical-radical reactions, electrophilic addition, and electron-transfer reactions [16]. At low or neutral pH values, these radical reactions are of minor importance regarding degradation reactions of micropollutants. One possibility to increase the concentration of highly-reactive $^{\bullet}OH$ radicals is ozonation at pH > 8, which is considered an AOP [17]. Other AOP examples include O_3/H_2O_2, O_3/UV, H_2O_2/UV, Fenton (Fe^{2+}/H_2O_2), photo-Fenton, electro-Fenton, chelating-agent-assisted Fenton/photo-Fenton, heterogeneous photo-oxidation using

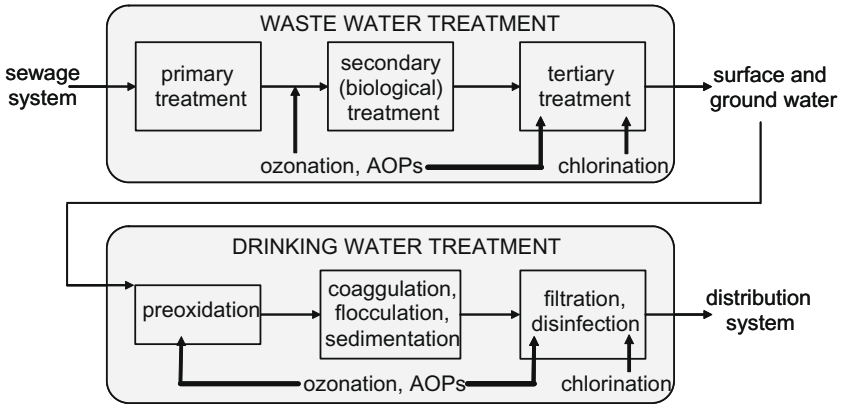

Figure 1. Possible applications of ozonation and advanced oxidation processes (AOPs) in treatment of wastewater and drinking water (adapted from [14]).

titanium dioxide (TiO_2), γ radiolysis, and sonolysis [16]. The versatility of AOPs is reflected in different options for producing $^{\bullet}OH$ radicals, by combining various chemical agents [e.g., O_3, hydrogen peroxide (H_2O_2), transition metals, and metal oxides] and auxiliary energy sources (e.g., UV-vis radiation, electronic current, γ-radiation and ultrasound). Hydroxyl radicals are considered the primary oxidants in AOPs, while other radical and active-oxygen species [e.g., superoxide radical anions ($O_2^{\bullet-}$), hydroperoxyl radicals ($HO_2^{\bullet}$), triplet oxygen ($^3O_2$), and organic peroxyl radicals ($ROO^{\bullet}$)] are also involved [16].

The main concern about application of these treatments is formation of various by-products as a consequence of the non-selectivity of $^{\bullet}OH$ radicals, that trigger complex, parallel, consecutive pathways of by-products. However, selective reactions of chlorination and ozonation have also proved to render persistent and even toxic intermediates [18,19], so disappearance of the original drug does not imply that the treatment was efficient. Some conventional parameters [e.g., total organic carbon (TOC), chemical oxygen demand (COD), dissolved organic carbon (DOC), absorbable organic halogen (AOX), and aromaticity] can be used to estimate the process, since, even when possible, complete mineralization does not seem to be cost effective.

Considering the potential hazards of by-products of pharmaceutical residues generated during chlorination, ozonation and AOP, their identification and quantification, as well as elucidation of main reaction mechanisms, are necessary for safe application of such processes for water treatment. These products may have preserved the mode of action of the parent compound or even be biologically more active, hence quantitative evaluation and determination of their radical rate constants would afford kinetic and mechanistic data for estimating efficiency in removing pharmaceuticals from real waters that contain high levels of dissolved natural organic matter (NOM) and other hydroxyl radical scavengers. Furthermore, in the cases where AOPs (e.g., TiO_2 and photo-Fenton photocatalysis) are combined with the biological treatment, the intermediates formed could be more resistant to degradation by activated sludge and/or inhibit the activity of microbial population [20,21].

Novel mass-spectrometry (MS) analyzers [e.g., (quadrupole) time-of-flight ((Qq)ToF) enabling accurate-mass measurements, linear ion trap (LIT) and hybrid quadrupole LIT (QqLIT) offering high-sensitivity multiple MS (MS^n) experiments, and LTQ Orbitrap combining both features] are powerful tools for identifying so-called ''known unknowns'' (i.e. transformation or degradation products of pharmaceuticals formed during treatment of drinking water and wastewater). Although these highly-sensitive, selective methods afford reliable results in the process of qualitative analysis, gas chromatography (GC) and liquid chromatography (LC)-hyphenated techniques are frequently engaged as complementary analytical tools [e.g., LC-nuclear magnetic resonance (NMR) spectroscopy, LC-ultraviolet (UV) detection, LC-infrared (IR) spectroscopy, GC-MS and LC-MS].

Given the importance of accurate identification of degradation products, we summarize major studies performed with ozonation, chlorination and AOP treatment of pharmaceuticals, including advanced MS methods and conventional detectors coupled to GC or LC. In contrast to previously published works on this subject [22,23], we primarily focus on the combined approach of using advanced MS methods for structural identification of oxidation intermediates of pharmaceuticals, and bioanalytical assays for evaluation of the toxicity of the newly identified products.

For a complete risk-assessment study on the transformation products (TPs) of pharmaceuticals formed during treatment of drinking water and wastewater, determination of their ecotoxicity is fundamental and a prerequisite for comprehensive protection of the environment. Since only a few published scientific papers encompass both aspects, we also discuss major studies on the elucidation of unknown products, in order to illustrate the advantages and drawbacks of different MS methodologies.

However, we do not discuss degradation products of pharmaceuticals formed during biological wastewater treatment (i.e. microbial metabolites), due to a complete lack of data on their ecotoxicity. Along with biodegradation processes, pharmaceutical residues can undergo complex enzymatic reactions that can result in microbial products with toxicity equal to or greater than that of the original, parent compound [23]. The absence of such studies is of major concern and future investigations should focus on complete evaluation of the hazards of biotransformation products.

2. GC and LC combined with conventional detectors and mass spectrometers

GC-MS has long been a method of choice for identifying volatile compounds in complex mixtures. However, since products of biological and oxidative transformation are often more polar than the original compound, GC-MS techniques frequently cannot cope with identifying them due to their poor volatility. Another major drawback is that GC-MS is unsuitable for the analysis of thermally-labile compounds. Moreover, the selectiveness of the derivatization step distinguishes potential new products with structures different from that of the target compound. Nevertheless, Zhang et al. [24] and Andreozzi et al. [25] used the full-scan electron impact (EI) mode of GC-MS to identify the reaction intermediates of degradation of acetaminophen by TiO_2 photocatalysis, UV/H_2O_2 and O_3. After derivatization of liquid samples

(i.e. silylation with BSA or BTSFA+TMCS), hydroxyl and carboxyl groups were converted into their volatile TMS-ether and TMS-ester derivatives.

GC-MS is frequently employed for detection of apolar degradation products, and/or as an identification tool complementary to LC-MS [26,27]. For example, Lambropoulou et al. [26] detected products of TiO_2 photocatalytic degradation of bezafibrate 4-isopropoxy-benzaldehyde, 4-chloro-benzaldehyde and 4-chloro-benzamide by fitting the recorded EI mass spectra using the NIST library. Of these three intermediates, only 4-chloro-benzamide was detectable by LC-ToF-MS, probably due to the low ionization efficiency, highly polar character and/or thermal instability and low volatility of the other two compounds. Pérez-Estrada et al. [27] managed to identify apolar degradates of diclofenac formed in the photo-Fenton treatment by employing GC-(EI)-MS. Furthermore, analysis in positive chemical ionization (PCI) mode with methane as the reagent gas enabled accurate confirmations of the molecular weights and detection of co-eluting compounds. The intermediate products identified did not pose the quinone imine group as determined for the primary degradation route of diclofenac, yet they mainly resulted from direct reaction of the aliphatic chain in the structure of the compound.

In ozonation experiments with carbamazepine, McDowell et al. [28] identified three TPs of carbamazepine [i.e. 1-(2-benzaldehyde)-4-hydro-(1H,3H)-quinazoline-2-one (BQM), 1-(2-benzaldehyde)-(1H,3H)-quinazoline-2,4-dione (BQD) and 1-(2-benzoic acid)-(1H,3H)-quinazoline-2,4-dione (BaQD)]. Oxidation-product BQD was sufficiently apolar and volatile to yield its GC-(EI)-MS spectrum, whereas additional fragmentation experiments were performed on GC-ion trap (IT)-MS. The fragmentation pattern of BQD was compared to fragmentations of comparable quinazoline compounds [i.e. 3-methyl-(1H,3H)-quinazoline-2,4-dione, a sex pheromone in the pale-brown chafer, and caffeine]. The major fragmentations of these compounds via a two-bond cleavage on their heterocyclic rings suggested nitrogen-driven and carbonyl-oxygen-driven α-cleavages at the hetero-ring during ozonation of carbamazepine. However, the structure of BQD could not be unambiguously elucidated from the MS data. In order to gain more information, other techniques were used (e.g., ^{1}H NMR, COSY, ^{13}C NMR and spin-echo experiments).

NMR spectroscopy (in the first place ^{1}H-NMR, ^{13}C-NMR and ^{15}N-NMR) is often combined with other GC-MS and LC-MS methods in qualitative analysis of pharmaceuticals. Frequently, the ^{1}H-NMR spectrum cannot provide unequivocal evidence of the structure, as was the case for the BQD-ozonation product of carbamazepine. The ^{13}C-NMR spectrum enabled assignments of chemical shifts produced from ^{13}C signals of the products dissolved in methylene chloride-D_2 and compared them to those obtained for the molecules containing quinazoline and benzaldehyde moieties. These chemical shifts exhibited great similarities, so the hypothesized structure of BQD was finally confirmed. Nevertheless, ozonation products BQM and BaQD could not be isolated for NMR measurements. The need to separate individual compounds without impurities represents a major drawback of NMR analysis, since in processes, such as chlorination, ozonation and AOPs, multiple degradation products will be formed.

Buth et al. [29] successfully combined ^{1}H-NMR and 2D-NMR spectroscopy with high-performance LC (HPLC)-ToF MS operated in electrospray ionization (ESI) mode and IR spectroscopy to characterize products isolated after chlorination of cimetidine. Mechanisms of chlorination were determined to proceed via cimetidine sulfoxide as the primary intermediate, rendering the same terminal products [i.e. 4-hydroxymethyl-5-methyl-1H-imidazole, 4-chloro-5-methyl-1H-imidazole, and either a ß-sultam (N-cyano-N'-methyl-N"-ß-sultamyl-guanidine) or a δ-sultam (N-(2-methyl-1,1-dioxide-1,2,4-thiadizinan-3-ylidene) cyanamide)], independently of pH. The first two products (i.e. cimetidine sulfoxide and 4-hydroxymethyl-5-methyl-1H-imidazole) were identified by matching their HPLC retention times with the authentic standard and ^{1}H-NMR spectra. Further, 4-chloro-5-methyl-1H-imidazole revealed a monochlorine isotopic pattern and ^{1}H-^{13}C correlations in positions very similar to those for the methyl and 2-position protons seen in the spectrum of 4-hydroxymethyl-5-methyl-1H-imidazole, obtained in 2-D heteronuclear multiple-bond correlation (HBMC) experiments using NMR spectroscopy. However, the methylene signal missing in the spectrum of chlorinated derivative indicated replacement of the hydroxylmethyl group with chlorine. Finally, the fourth product could not be unequivocally identified as ß-sultam or δ-sultam by the available spectrometric and spectroscopic techniques. The peak recorded in ESI(+) mode corresponded to the sodium adduct, $[M+Na]^+$ 211.0244, which, after H/D-exchange (use of D_2O as HPLC solvent instead of water) appeared at m/z 214.0. The three acid protons exchanged were assigned to the proton on the secondary amine and two protons at the α-C-atom to the sulfonamide functionality. When employing chemical ionization (CI) instead of ESI, a fragment ion at m/z 64 was detected, probably resulting from the loss of SO_2. Further evidence for the sultam structure of this intermediate was provided by its ^{1}H NMR and IR spectra, although without the possibility of distinguishing between the ß isomer and the δ isomer. Nevertheless, this product was somewhat unexpected as the outcome of chlorination, since it resulted from C-S cleavage, intramolecular nucleophilic substitution and oxidation.

Another study from Dodd and Huang [30] illustrated the importance of combining supplementary analytical

techniques. In the reaction of sulfamethoxazole with free chlorine, degradation product N-chloro-p-benzoquinoneimine (NCBQ) with potentially higher acute toxicity than the parent compound was detected by ^{1}H-NMR and GC-MS, yet it yielded no signal in positive ESI or atmospheric pressure chemical ionization (APCI) modes of LC-MS analysis.

Secondary oxidation products of pharmaceuticals (e.g., phenols and acids) can usually be identified by simple detectors [e.g., UV, fluorescence (FLD) and diode array (DAD)]. Using HPLC-DAD and HPLC-FLD, Doll et al. [31] identified 4-chlorophenol, hydroquinone and isobutyric acid as degradation products of clofibric acid in TiO_2 suspensions. However, primary degradation products 2-(4-hydroxyphenoxy)-isobutyric acid (m/z 195), hydroxyisobutyric acid (m/z 103) and 4-chlorohydroxyphenol (m/z 143, 145, ratio 3:1) were tentatively identified by HPLC-triple quadrupole (QqQ)-MS.

In another study from the same authors [32], the TiO_2 photocatalytic degradation product of carbamazepine – 10,11-dihydro-carbamazepine-10,11-epoxide – was identified by its LC retention time and UV spectrum, based on comparison with authentic standards. Other degradates (i.e. hydroxycarbamazepine and dihydroxycarbamazepine, acridine derivatives) for which no authentic standard was available were characterized by their tandem MS (MS^2) spectra obtained using LC-QqQ-MS.

For determination of chlorination products of acetaminophen, Bedner et al. [18] engaged two LC-UV systems, one with electrochemical (EC) and other with MS detection. In the full-scan performed in ESI(+) mode at LC-UV-MS, product N-acetyl-benzoquinone-imine (NAPQI) emerged as a methanol adduct $[M+H+MeOH]^+$ 182.1, while the molecular ion $[M+H]^+$ 150.1 was less intense. This spectrum matched that obtained for a standard of NAPQI, which, together with the equivalent retention times obtained at LC-UV-EC for the authentic standard and the sample, confirmed the identity of this product. The mass spectrum of the second degradation product of acetaminophen – 1,4-benzoquinone – could not be obtained in the ESI mode, whereas, in the APCI mode, one ion was seen in the spectra of both sample and the standard of 1,4-benzoquinone, at m/z 108.1. Since the nominal mass of 1,4-benzoquione is 108.0, the ion was explained by either electron capture to form a radical anion or by a mass gain that was exactly balanced by a mass loss to make a negative ion. Also, the retention times recorded by LC-UV-EC for the sample and the standard were identical. Furthermore, the most prominent product in the spectrum was detected with the molecular ion $[M+H]^+$ 186.1, which exhibited a monochlorinated pattern with the second ion appearing at m/z 188.1. The combination of EC detection with iodide-post-column reaction chemistry [33] allowed exclusion of any possible chloramides, and that suggested that the $[M+H]^+$ 186.1 corresponded to the products obtained by chlorination of the aromatic ring, probably in the *ortho* position to the phenol group, thus affording chloro-4-acetamidophenol. Dichlorinated acetaminophen was also recognized from its characteristic isotopic pattern with $[M+H]^+$ 220.0 and additional ions at m/z 222.0 and 224.1, whereas ammonium and sodium adducts were detected at m/z 237.0 and 239.0.

3. LC-MS methods based on MS^n experiments

Having a structure similar to that of the parent compound, TPs are not complete unknowns. Their structures are elucidated by comparing mass spectra of analyte and its TPs, considering possible molecular changes relative to the parent compound and using putative transformation pathways. To facilitate the identification process, derivatization of functional groups of the products formed and/or H/D-exchange experiments can also be employed [34,35]. Nevertheless, lack of analytical reference standards means that accurate quantification of degradation products of pharmaceuticals is rarely possible.

IT-MS has proved to be a very useful analytical tool, due to its ability to determine multi-stage fragmentation pathways of molecules through MS^n experiments. In the trap comprising two hemispherical electrodes and a ring electrode, IT-MS can trap and accumulate ions that are further focused toward the centre of the trap by using an oscillating voltage. This increases the signal-to-noise (S/N) ratio, although it entails some drawbacks (e.g., small trapping volume, loss of the dynamic range response due to space charging, and overfilling of the IT), which result in deterioration in the mass spectrum [36]. The major advantages of LIT over IT are larger ion-storage capacity and higher trapping efficiency. The QqLIT (i.e. QTRAP-MS) offers an additional possibility to operate the third quadrupole as a normal quadrupole or in the LIT mode.

The advantage of the MS^n capability of LIT-MS was nicely illustrated in studies on the identification of products of ozonation, TiO_2 and UV/TiO_2 photocatalysis of ciprofloxacin [37,38], and TiO_2 photocatalysis of analgesic anxiolytic drug buspirone [39] and anti-inflammatory drug diclofenac [40]. Paul et al. [37] used LC-(ESI+)-MS^2 analysis with an IT instrument to identify six degradation products of UV and visible-light TiO_2 photocatalytic degradation of ciprofloxacin; all six degradation products retained the oxoquinoline carboxylic acid group. Also, De Witte et al. [38] determined the ozonation-degradation pathway of ciprofloxacin by LC-(UV)-IT-MS operating in low-resolution MS (LRMS) and high-resolution MS (HRMS) modes. Collision-induced dissociation (CID)-MS fragmentation revealed characteristic losses of isatin analogues (i.e. CO and C_2O_2), indicating the presence of a diketone. However, in the

MS^2 spectra obtained for anthranilic-acid analogues, losses of H_2O, H_2O and CO, and H_2O and C_2O_2 were recorded, whereas the hypothesized structures were tentatively identified by comparison with the spectrum of analogous N-formylanthranilic acid. Whereas isatin and anthranilic-acid analogues were derived from degradation of the quinolone moiety of ciprofloxacin, oxidation reactions also occurred at the piperazinyl fraction, with the main degradation product formed through a net loss of C_2H_2, desethylene ciprofloxacin. Desethylene ciprofloxacin was univocally identified based on nominal mass and HPLC retention time. All products were completely mineralized during UV photocatalysis, whereas, in the visible-light assisted process, the fluoroquinolone-core structure was possibly preserved. However, whether the degradation of ciprofloxacin will occur primarily at the carboxylic group (quinolone moiety) with formation of isatin and anthranilic acid analogues, or at the piperazinyl substituent will depend on the pH of the solution. In the first case, at neutral pH, carboxylic and keto groups, which are considered necessary for binding quinolones to the DNA gyrase target, are degraded [41]. However, if the ozonation is conducted at pH 3 or pH 10, intermediates formed preserve the essential structure of antibacterial quinolone, whereas the data on the activity of desethylene ciprofloxacin reported in literature are still contradictory [42–44]. This stresses the importance of optimizing ozonation in treating water loaded with quinolones.

Calza et al. [39] identified several intermediates of TiO_2-photocatalytic degradation of buspirone, which were also found in the *in vivo* experiments on rats and horses. Buspirone and its degradation products were characterized by MS^n experiments, conducted on a LC-(ESI)-IT-MS instrument, by linking the main fragments in the fragmentation pathway for buspirone shown in Fig. 2. In particular, the product ion at m/z 122 will be indicative of the unchanged pyrimidine substructure, while the m/z 222 and m/z 180 ions are diagnostic of the unchanged azaspirone-decane-dione substructure.

In another study published by the same authors [40], the same methodology was used to identify several hydroxyl and dihydroxy derivatives formed during TiO_2 photocatalytic treatment of diclofenac, which further transformed into chlorophenol or hydroxylphenol products. Four products holding molecular ion $[M+H]^+$ 312 were detected, exhibiting the same characteristic losses of water, formic acid and joint losses of formic acid and chlorine radical as those observed in the fragmentation pathway of diclofenac. It was therefore deduced that the hydroxylation took place at the aromatic rings. The discrepancies in the MS^3 spectrum of the fourth product with $[M+H]^+$ 312 relative to the above-mentioned compounds situated the hydroxyl group at the lateral chain of diclofenac. A product having 2 Da less than the monohydroxylated derivatives pointed to a quinine-imine transformation. Two dihydroxylated derivatives with $[M+H]^+$ 328 and $[M+H]^+$ 284 were also identified, generated by $^{\bullet}OH$ radical attack on hydroxyl-diclofenac and consequent decarboxylation, respectively.

Although the usual operating mode of MS analyzers is ESI due to enhanced detection of polar compounds, several studies [45,46] used the APCI interface, which is suitable for less polar, thermally inert compounds. Calza et al. [45] identified hydroxylated and R-NH_2 derivatives formed in TiO_2-photocatalytic degradation of sulfonamide drugs (i.e. sulfadiazine, sulfamerazine, sulfadimethoxine and sulfathiazole) by MS^2 experiments performed on an LC-(APCI)-IT-MS instrument. Moreover, one of the intermediates identified for sulfamerazine – 4-methyl-2-aminopyrimidine – was stable in the degradation time investigated (i.e. 30 min). Furthermore, APCI was used to identify ozonation intermediates of tetracycline, because typical conditions of this ionization can prevent interface obstruction usually caused by the required use of oxalic acid (a non-volatile compound) [46].

4. LC-MS methods based on accurate-mass measurements

ToF-MS represents an indispensable analytical tool for the non-target screening and structural elucidation of metabolites and TPs, due to its full-scan sensitivity, high selectivity (lack of interferences) and specificity (correct empirical formula assigned), given by the high mass resolution and mass accuracy of ToF analyzers. It is based on the acceleration of ions by an electric field, whereas the time that ions need to reach the detector will depend on their kinetic energy, and thus their m/z ratios. When a ToF-MS is interfaced with commonly used continuous ion sources (e.g., ESI), the ions are introduced into the mass analyzer in a direction perpendicular to the direction of flight and accelerated down the ToF flight tube in a pulsed fashion. This orthogonal accelerating ToF (oaToF)-MS has high mass accuracy (generally within a few parts per million (ppm) of the exact m/z values calculated from the nuclide masses and the ionic charge z), resolution of 10 000–20 000 (FWHM) and allows rapid mass scanning in a theoretically unlimited mass range [47]. In a QqToF instrument, the precursor ion is selected in a quadrupole mass fitter and dissociated in a radiofrequency (RF)-only multipole collision cell, and the resultant fragments are analyzed in a ToF-MS instrument. A CID spectrum with accurate masses of both precursor and product ions is therefore impossible with LRMS analyzers. However, one of the greatest drawbacks of this instrument is low ion transmission (resulting in poor MS^2 sensitivity and detection limits) and a limited intensity range over which accurate-mass data can be acquired.

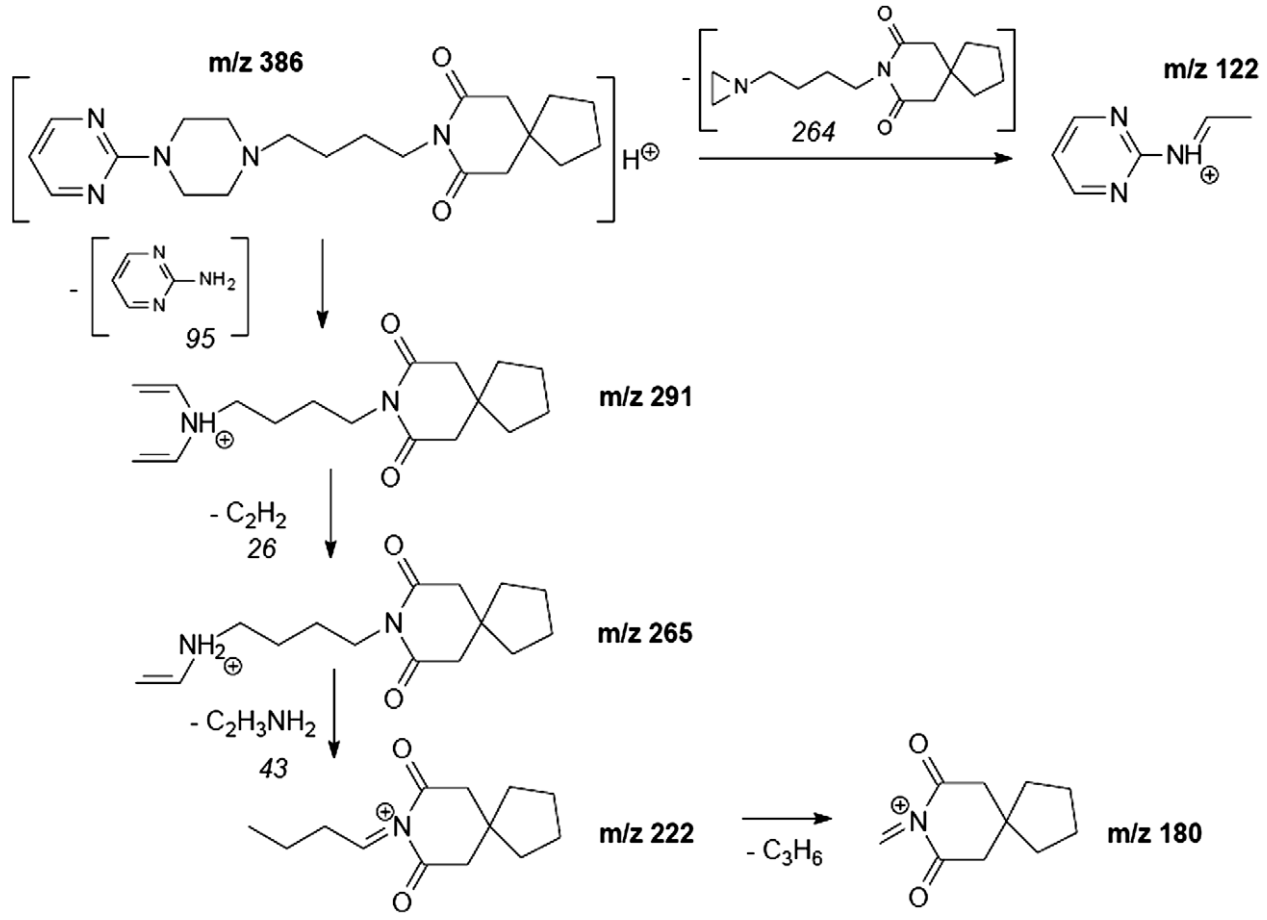

Figure 2. Fragmentation pathway followed by buspirone (reproduced from [39] with permission of Elsevier).

In our own works, we identified intermediate products of TiO_2 and photo-Fenton treatment of ß-blocker atenolol and anti-histaminic drug ranitidine solely by ultra-performance LC (UPLC)-(ESI+)-QqToF-MS [48,49]. We elucidated the structures and interpreted the fragmentation pathways of atenolol, ranitidine and the detected TPs acquired in CID MS^2 experiments under optimized conditions of collision energy (CE) and cone voltage (CV). The unequivocal identification of the degradation products was facilitated by the MassLynx V4.1 software identification program of the QqToF instrument with a mass-measurement-accuracy threshold of 5 ppm. Interpretation of the fragmentation pathways of the compounds detected was mainly supported by the analogies and the differences with the MS^2 spectra of original compounds and the oxidation reactions expected in the processes investigated.

In photocatalytic experiments with ranitidine [48], a product having a molecular ion $[M+H]^+$ 286, denominated as P285, was hypothesized to be formed by consecutive cleavages of the N,N-dimethyl amino moiety and $^{\bullet}OH$ radical attack on the terminal methyl group substituent, followed by addition of oxygen. By comparing the fragments of P285 with that of ranitidine, mutual loss of 46 Da was detected, corresponding to the loss of the $NO_2^{\bullet}$ radical. The rupture of the C-S bond led to the formation of a methylated furan-aldehyde fragment ion at *m/z* 109, similar to the fragment ion *m/z* 138 formed in the case of ranitidine. A degradation product carrying a molecular ion $[M+H]^+$ 270.0900 was then assumed to be formed by photocatalytic cleavage of oxygen from the nitrite group ($-NO_2$) in product P285, and that was confirmed by the absence of the characteristic loss of 46 Da. The absence of typical loss of N,N-dimethyl amino moiety in product P300 ($[M+H]^+$ 301.1362) suggested cleavage of the terminal methyl group in the tertiary amine function. Next, three more peaks detected in the full-scan mode of QqToF instrument were assigned to hydroxylated derivatives of ranitidine and their quinone-imine analogues. These products had molecular ions $[M+H]^+$ 331.1423, 345.1266 and 361.1145, which corresponded to one more oxygen atom, two more oxygen and two less hydrogen atoms, and three more oxygen and two less hydrogen atoms relative to ranitidine, respectively. Their peculiar MS^2 fragments were linked together in a frag-

mentation pathway, whereas both fragment ions and radical fragment ions were confirmed by rational and integer double-bond equivalent (DBE) values, respectively.

The same approach was applied when elucidating the structures of degradation products of atenolol [49] (see Fig. 3). The difference in mass of 29 Da between product P237 ($[M+H]^+$ 238.1444) compared with the molecular ion of atenolol ($[M+H]^+$ 267.1702) was assumed to be due to the loss of an amide group from the molecule and addition of oxygen to the alkyl group attached to the ring after hydrogen abstraction by $^{\bullet}OH$ radical attack, resulting in a keto derivative. In the MS^2 spectrum of both compounds, characteristic losses of isopropyl and amino isopropyl groups and water were observed. Two intermediates with molecular ions $[M+H]^+$ 283.1656 (P282) and 281. 1505 (P280) corresponded to a monohydroxylated atenolol and its quinone-imine derivative, respectively. Again, a characteristic loss of the isopropyl group (42 Da) in the spectra of P280 and 282 afforded fragment ions *m/z* 239 and 241, respectively. These fragments further exhibited consequent losses of acetamide moiety, water and ammonia. The fragment ion at *m/z* 133.028 in the fragmentation pattern of P280 was possibly formed by the loss of the methyl-isopropylamine group, water and the acetamide moiety from the molecular ion, and intramolecular cyclization afterwards. Besides these products, at retention times 2.5 min, 4.3 min and 5.15 min, three peaks with the same molecular ion $[M+H]^+$ 254 were detected. Since they presented the same losses in the mass spectra with the same relative ion-signal intensities, they were all labeled as P253, whereas the non-specific $^{\bullet}OH$ radical attack on the P237 intermediate was assumed to be responsible for their formation. Since there were only two available positions for the addition of the $^{\bullet}OH$ radical, *ortho*- and *meta*-, to the aldehyde group, three different peaks could be explained by the intramolecular hydrogen bond between the hydrogen of the –OH group attached to the ring and oxygen of the aldehyde group (*ortho* isomer) or the absence of one (*meta* isomer). It could be assumed that, in the case of the *meta* isomer, the hydrogen bond with the ether oxygen from the alkyl backbone would be less probable since the electron density at ether oxygen is lowered by the alkyl substituent. The presence of intramolecular hydrogen bond has been previously reported for *ortho* isomers of hydroxylated photocatalytic intermediates of bezafibrate [26], whereas an increase in retention time was observed due to the decrease in polarity of the molecule. Thus, the most polar compound eluting at 2.5 min was assigned to *meta*-hydroxylated intermediate P253, while the compounds appearing at 4.3 min and 5.15 min were possibly the two *ortho* derivatives, without and with the intramolecular hydrogen bond, respectively. Finally, the *m/z* 116 fragment ion, obtained by breaking the C-O bond was observed for all intermediates encountered, indicating an intact isopropyl moiety (see Fig. 3).

In several studies, exact-mass assignment to TPs available with ToF-MS was combined with GC-(EI)-MS in order to determine the entire degradation pathways of pharmaceuticals, including polar, less polar and/or apolar products [26,27,50]. Pérez-Estrada et al. [50] elucidated structures of several degradation products of analgesic drug dipyrone, formed during TiO_2-assisted and photo-Fenton photocatalysis. GC-MS analysis enabled identification of five intermediates, which were tentatively identified by their full-scan mass spectra. Four products were formed by an $^{\bullet}OH$ radical attack on the double bond in the heterocyclic ring and had some common fragments (*m/z* 121, 107, 92 and 77). The fifth product detected by GC-MS preserved the heterocyclic ring, while the other five degradation products having the heterocyclic ring were identified by LC-(ESI)-ToF-MS. Since there was no possibility of performing CID experiments, the proposals for chemical structures of these compounds were based on their accurate masses measured for the molecular ions (error <5 ppm), oxidative process chemistry and DBE data given by the software. Moreover, the amounts of nitrate and ammonia determined by ion chromatography (IC) provided additional information for hypothesizing a possible oxidation pathway of dipyrone.

In another study from the same authors [27], the combination of GC-MS and LC-ToF-MS was engaged in identifying the photo-Fenton intermediates of diclofenac. Again, apolar degradation products were determined based on their full-scan EI spectra matching with spectral libraries or by their fragmentation patterns, whereas semi-polar and polar products were analyzed by HPLC-(ESI)-ToF-MS. The two early appearing peaks with molecular ions $[M+H]^+$ 312.0193 and 310.0031 corresponded to one more oxygen, and one more oxygen and two hydrogen less compared to the diclofenac molecule, respectively. This suggested that a hydroxyl group was attached to the aromatic ring, whereas the second product corresponded to its quinone-imine derivative. Based on the measured masses of protonated molecules, as well as frontier electron density (FED) theory [which predicts sites of $^{\bullet}OH$ radical attack by calculating the higher molecular orbital (HOMO)], formulae for other intermediate products were proposed, while the resulting accurate-mass errors were always <2.5 ppm. The accuracy of the ToF instrument was enhanced by internal calibration, whereby internal references were introduced with a dual-nebulizer ion source at a very low flow rate, with constant autocalibration and recording of reference mass along with the raw data.

Lambropoulou et al. [26] used GC-MS, HPLC-ToF-MS and HPLC-DAD to identify up to 17 degradation products of TiO_2 photocatalysis of bezafibrate under simulated solar light. LC-ToF analysis was able to detect

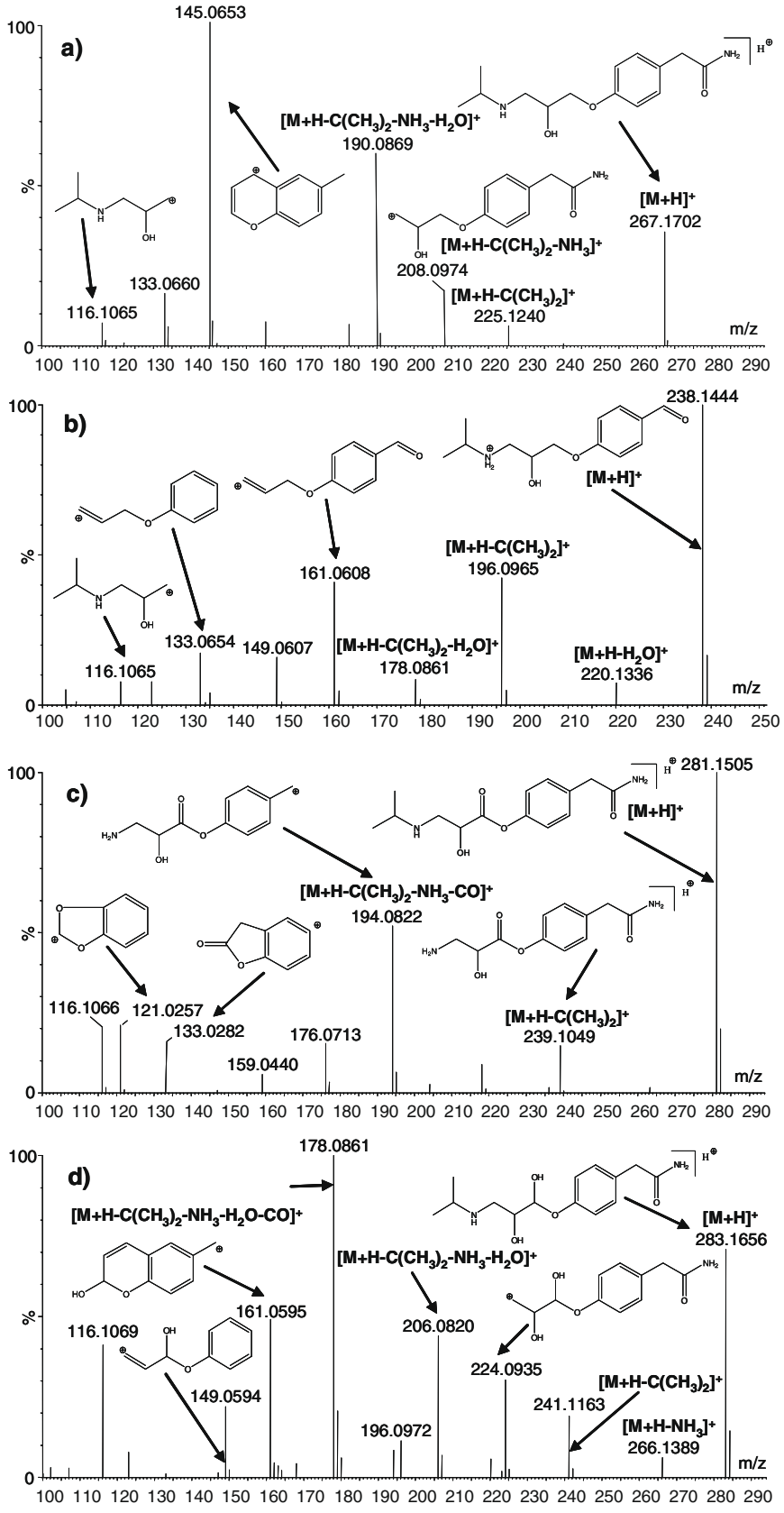

Figure 3. Spectra obtained in ESI(+)-MS^2 experiments on a QqToF instrument (cone voltages 25 V, collision energies 15–25 eV) for atenolol and the intermediate products of its photocatalytic degradation: a) atenolol; b) P237; c) P281; and, d) P283 (reproduced from [48] with permission of Elsevier).

various hydroxylated products in the first stage of the treatment, based on accurate-mass measurement of protonated molecules, abundances of the chlorine isotope in the molecular ions, characteristic fragment ions used as diagnostic ions, and, when possible, accurate-mass measurements of sodium adducts of molecular ions. A fragment ion from the spectrum of bezafibrate (Cl^{35} $[M+H]^+$ 362.1154, Cl37 $[M+H]^+$ 364.1128) exhibiting a chlorine-isotope pattern at *m/z* 138.9965 and 140.99 was used for diagnosis. The software tool calculated a unique elemental composition corresponding to this diagnostic ion, C_7H_3ClO, whose structure is shown in the inset in Fig. 4. Targeting the *m/z* of the diagnostic ion, numerous chlorine-containing products were found in the total ion chromatogram (TIC). Several monohydroxylated products were detected, as a consequence of $^{\bullet}OH$ radical attack on the 4-chlorobenzoyl ring or the phenoxy moiety. Interestingly, two peaks that eluted prior to bezafibrate at 19.7 min and 20.9 min had identical mass spectra and the same molecular ion $[M+H]^+$ 378.1100. From the best-fit formula given by the software and considering the activating effect of the R-oxy group of bezafibrate on the aromatic ring, these two products were identified as monohydroxylated derivatives (*meta*- and *ortho*- at 19.7 min and 20.9 min, respectively). In this case, consideration of their polarity, which determined the order of elution, helped assign the peaks to their corresponding isomers. Namely, the *ortho* isomer assumed an intramolecular hydrogen bond between the hydrogen of the hydroxyl group borne by the ring and the oxygen of the ether group.

The latest advances in MS are LTQ Orbitrap and Fourier transform (FT)-MS. Next-generation FT ion cyclotron resonance (FT-ICR)-MS accumulates ions externally to a superconducting magnet, and, unlike other MS techniques where ions are detected by hitting a detector (e.g., electron multiplier), in FT-ICR, ions only pass near detection plates, and the *m/z* ratio of ions is determined based on the cyclotron frequency of the ions in a fixed magnetic field [51]. Besides the high trapping capacity and MS^n capabilities, FT-ICR has the automatic gain control (AGC) of LIT-MS with unsurpassed mass accuracy, fast data collection, good sensitivity, good dynamic range and high resolution, although the high

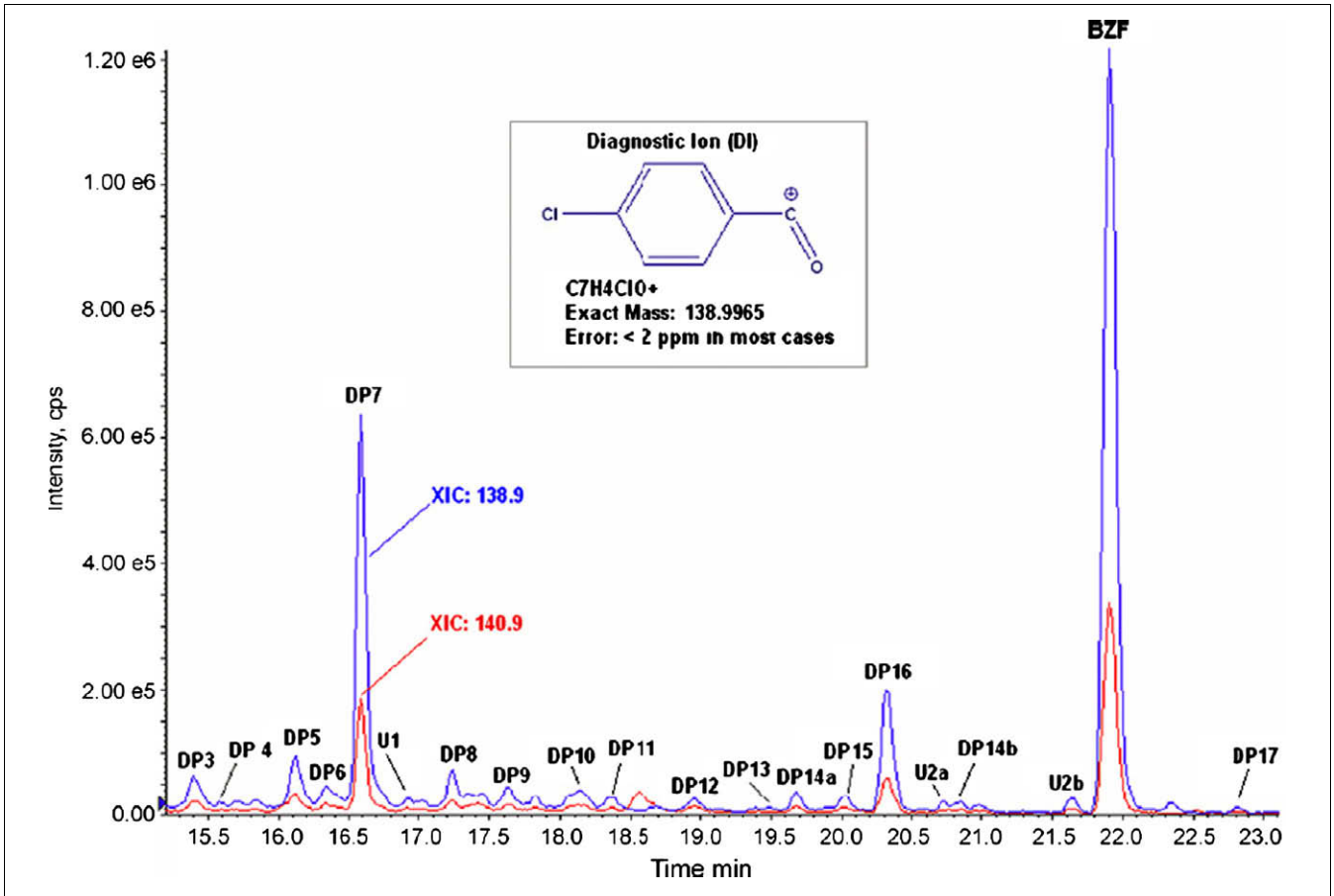

Figure 4. Total ion chromatogram (TIC) by LC-ToF-MS obtained from an SPE extract of bezafibrate solution after 60 min of irradiation with simulated solar light in the presence of TiO_2 suspension (100 mg/L). The TIC shows the protonated molecular ion of bezafibrate at *m/z* 362 and chlorinated by-products. Identification criteria for chlorine by-products: (i) searching of diagnostic ion-accurate mass 138.9965 (remaining fragment from bezafibrate); and, (ii) chlorine isotopic profile (reproduced from [26] with permission of Elsevier).

cost of these instruments limits wider application in environmental and pharmaceutical laboratories [52].

Due to the high cost of FT-ICR spectrometers, LTQ Orbitrap is considered a good alternative because of its high resolution and good mass accuracy [52]. The LTQ Orbitrap is a hybrid MS combining LIT and Orbitrap, enabling excellent mass resolution and accuracy, as well as high sensitivity. The ions are introduced tangentially into the electric field between the inner spindle-like electrode (central electrode) and an outer barrel-like, coaxial electrode, and trapped because their electrostatic attraction to the inner electrode is balanced by centrifugal forces. Ions of a specific m/z ratio therefore move in rings that oscillate along the central spindle, while the frequency of these harmonic oscillations is independent of the ion velocity and inversely proportional to the square root of the m/z ratio.

As demonstrated by recent publications [53,54], the LTQ Orbitrap mass analyzer supports qualitative analysis of degradation products of pharmaceuticals present at trace-level concentrations. Seven intermediate products of salbutamol in TiO_2-assisted photocatalysis were structurally elucidated by LC-LTQ Orbitrap-MS, by taking into account their retention times, kinetics of evolution and exact-mass measurements of the MS and MS^n spectra [54]. Characteristic fragment ions in the spectrum of salbutamol ($[M+H]^+$ 240.1594) were obtained by the loss of water (m/z 222.1489), *tert*-butene (m/z 166.0863) and again water (m/z 148.0757). The species having molecular ions $[M+H]^+$ 210.1489 and 226.1438 exhibited the same *tert*-butene and water losses, but the characteristic loss of hydroxylmethyl group was absent. These products were identified as 2-(*tert*-butylamino)-1-(3,4-dihydroxyphenyl)ethanol and 2-(*tert*-butylamino)-1-(4-hydroxyohenyl)ethanol. Two species with the same nominal mass were identified as molecular ions $[M+H]^+$ 224.1654 and 224.1281, products of the cleavage of one hydroxyl group and methylic group, respectively. The first, $[M+H]^+$ 224.1654, presented the same peculiar losses of *tert*-butene and water, whereas the second, $[M+H]^+$ 224.1281, followed a different fragmentation pathway and had a shorter retention time than the parent compound, in accordance with the loss of a methylic group. Three more products were observed, having molecular ions $[M+H]^+$ 182.1176, 118.1226 and 132.1019.

Medana et al. [53] used an LTQ Orbitrap for structurally elucidating products of the photocatalytic transformation of atenolol. Six species with molecular ions $[M+H]^+$ 283.1658 were detected, corresponding to monohydroxylated derivatives of atenolol as a consequence of non-selective $^{\bullet}OH$ radical attack. The exact positions of the attacks were determined by comparing their fragmentation pathways to that elucidated for atenolol. For example, for one of the monohydroxylated derivatives, besides neutral losses of water and *para*-hydroxyphenylacetamide mutual with the parent compound, unusual loss of methanol was seen, suggesting that one of the methyl groups was hydroxylated. Also, two other compounds, having molecular ions $[M+H]^+$ 283.1658, exhibited a fragmentation pattern similar to that recorded for atenolol, but with m/z values of fragments 15.9949 units higher. This implied insertion of a hydroxyl group into the aromatic ring at two positions, which afforded two isomers of monohydroxylated derivatives. Another pair of isomers with molecular ions $[M+H]^+$ 283.1658 was formed by attaching the hydroxyl group on the side-chain of atenolol, which exhibited the same characteristic losses of propene, isopropylamine and N-(1-methyl-2-hydroxyethyl)-N-(2-hydroxyethyl)-amine, whereas the latter loss excluded the $^{\bullet}OH$ attack on the aromatic ring. Since dihydroxylated oxidation products of atenolol were formed in small quantities, only MS^2 fragmentation of this compound could be performed on the LTQ Orbitrap, which impeded accurate attribution of $^{\bullet}OH$ radical-attack sites. Finally, six trihydroxylated intermediate products with molecular ions $[M+H]^+$ 315.1551 were detected, while their identification was facilitated by analogies with the MS^n spectra of the monohydroxylated and dihydroxylated derivatives and atenolol, and some characteristic losses (e.g., one loss of water indicated attachment of an –OH group into the aromatic ring and loss of allyl alcohol insertion of an –OH group into the propyl chain).

5. Toxicity in degradation/transformation studies

In published studies about TPs of pharmaceuticals, toxicity was generally taken as the overall toxicity of the solution (i.e. mixture of intermediates and possibly parent compound) by the Microtox test (see Table 1) [40,50,53–57]. The Microtox test measures the decrease in bioluminescence of the marine bacterium *V. fischeri*, as a result of inhibiting bacterial luciferase upon contact with toxic substances. This test is frequently used in the environmental studies, since it is simple, fast, sensitive and reproducible.

Calza et al. [40,57] followed the evolution of the toxicity of solution of diclofenac and imipramine during TiO_2-photocatalytic treatment by using the Microtox bioassay. In both studies, there was a maximum inhibition (expressed as % of inhibition of bioluminescence of bacteria) of 72% (after 20 min) and 83% (after 15 min) for diclofenac and imipramine solution, respectively. These maxima corresponded to the maximum concentrations of identified TPs, thus indicating that intermediates more toxic than imipramine were formed, although it was not possible to identify their individual toxicities. In the following period, the observed toxicities of the solutions decreased, yet remained at values higher than the initial toxicities of diclofenac and imipramine.

Table 1. Summary of studies that combine qualitative analysis of degradation products of pharmaceuticals in chlorination, ozonation and advanced oxidation processes (AOPs) with evaluation of the toxicity

Pharmaceutical, treatment	Transformation products	Analytical method	Toxicity	Toxicity test	Ref.
Acetaminophen[1], chlorination	NAPQI[2], 1,4-benzoquinone[3] mono- and dichlorinated derivatives	HPLC/UV/EC, HPLC/UV/MS	500 mg/kg[1] 20 mg/kg[2] 8.5 mg/kg[3]	Intraperitoneal injection in mouse	[18]
Cimetidine[1], Chlorination	Cimetidine sulfoxide[2] 4-hydroxymethyl-5-methyl-1H-imidazole[3] 4-chloro-5-methyl-1H-imidazole[4] β-sultam[5] δ-sultam[5]	HPLC-(ESI)-ToF MS, ^{1}H, 2D-NMR, IR	35 μg/L[1,a] 370 μg/L[2,b] 20 μg/L[3,a] 6.5 μg/L[4,a] 630 μg/L[5,b]	ECOSAR (daphnid or green algae)	[29]
Diclofenac, TiO_2 photocatalysis	mono- and dihydroxylated derivatives, 5-hydroxy diclofenac and its keto derivative, chloro- and hydroxyphenol derivatives 2,6-dichlorophenol, 4-chlorocathecol	HPLC-IT-MS	72%[c] max. (after 20 min)	Microtox (*Vibrio fischeri*)	[40]
Dipyrone (MAA), TiO_2 photocatalysis Photo-Fenton photocat.	4-aminoantipyrin, aniline, derivatives of pyrazole ring opening	GC-MS, HPLC-(ESI)-ToF-MS	<50% [c] (TiO_2) ~55-60% [c] (photo-Fenton)	Microtox (*Vibrio fischeri*)	[50]
Atenolol, TiO_2 photocatalysis	mono- and dihydroxylated derviatives (hydroxylation of benzene ring and alkyl side-chain)	HPLC-LTQ Orbitrap	-15% [c] (15-60 min)	Microtox (*Vibrio fischeri*)	[53]
Salbutamol, TiO_2 photocatalysis	2-(*t*-butylamino)-1-(4-hydroxylphenyl) ethanol, 2-(*t*-butylamino)-1-(3,4-dihydroxyphenyl) ethanol, 2-(*t*-butylamino)-1-(4-hydroxyl-3-methylphenyl) ethanol, 2-(*t*-butylamino)-1-(3,4-dihydroxyphenyl) ethanone, 2-(methylamino)-1-(3,4-dihydroxyphenyl) ethanone 2-(*t*-butylamino)-ethanol, 2-(*t*-butylamino)-acetic acid	HPLC-LTQ Orbitrap	54% [c] (after 15 min)	Microtox (*Vibrio fischeri*)	[54]
Ibuprofen, TiO_2 photocatalysis	monohydroxylated derivatives (hydroxylation of methylpropyl phenyl and arylcarboxylic moiety)	HPLC-(ESI)-ToF-MS	~92%[c] (after 120 min for 2-8 mg/L O_2; and 240 min for 40 mg/L O_2)	Microtox (*Vibrio fischeri*)	[56]
Imipramine, TiO_2 photocatalysis	mono-and polyhydroxylated derivatives, derviatives with cleaved aminoalkylic side-chain	GC-MS, HPLC-(ESI) QqQ-MS	83%[c] (after 15 min)	Microtox (*Vibrio fischeri*)	[57]
Bezafibrate, Ozonation	derivatives of benzene ring opening, trihydroxylated products, derivatives with cleaved non-chlorinated benzene ring	HPLC-MS	~0.09[d] max. (after 5-7 min)	Microtox (*Vibrio fischeri*)	[55]
Nitrofurazone[1], Chlorination	NFA[2], NFOA[3], HMF, HFA, chlorinated products	HPLC-UV	192[1,e], 2.64[2,e], 0.14[3,e]	Ames test (*Salmonella Typhimurium* TA100, without S9 mix)	[70]
Sulfamethoxazole, Ozonation	derivative of C-N bond cleavage, methanol, ethanol, phenol	GC-MS, FTIR	changes in cell's morphology	mammalian cell line (HepG2 cells)	[77]
Clarithoromycin, ozonation	clarithromycin-N-oxide demethylated clarithromycin deaminated clarithromycin acetalized clarithromycin	HPLC-(ESI)-MS^2, ^{1}H-NMR	~25 % of EC_{50} of clarithromycin	*P.putida* growth inhibition test	[83]

[a]PNEC derived from LC_{50}.
[b]PNEC derived from EC_{50}.
[c]% of inhibition Vibr. Fischeri.
[d]$1/EC_{50,15min}$.
[e]net reverants/nmol. NAPQI- N-acetyl-benzoquinone-imine, MAA- 4-methylaminoantipiryne (hydrolytic product of dipyrone), NFA- 5-nitro-2-furaldehyde, NFOA- 5-nitro-2-furoic acid, HMF- 5-hydroxymethylene-2-(5H)-furanone, HFA-5-hydroxy-2-furoic acid.

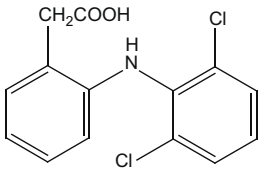

Dantas et al. [55] investigated the toxicity of the ozonated solution of bezafibrate by using *V. fischeri* strains, and expressed it in ''effect concentration'' ($EC_{50,15min}$) values (percentage of initial dilution, % v/v, that causes a 50% reduction of bacteria bioluminescence in 15 min). After a sharp increase in toxicity in the first 5–7 min, inhibition of bacteria slowly decayed reaching a value lower than that initially measured for bezafibrate solution after 105 min of ozonation.

In another study, the same authors [58] monitored the abatement and the changes in acute toxicity of bacteriostatic, sulfonamide-type antibiotic sulfamethoxazole during ozonation. The toxicity profile determined from the EC_{50} values calculated showed an increase in acute toxicity in the first 30 min of ozonation, reaching the initial value of sulfamethoxazole at the end of the experiment (1 h). This indicated formation of intermediates that were more toxic than the original drug. Furthermore, poor mineralization (only 18% of TOC removed) attained after 1 h of ozonation indicated that by-products formed towards the end of the reaction time were not susceptible to O_3 attack. These end-products were probably of lower aromatic character (e.g., aldehydes, ketones and organic acids), since the UV_{254} absorbance removal recorded was >80%. Additionally, biodegradability, measured as biological oxygen demand (BOD_5)/COD ratio was constantly increasing, changing from 0 to 0.28 in the time span of the experiment.

Medana et al. [53] also applied a Microtox assay to evaluate the toxicity of TiO_2-photocatalytic products of atenolol. The initial toxicity of atenolol solution showed a negative inhibition value of 15%, due to a bioluminescence-stimulation effect, known as hormesi [59]. During the first 60 min of bioassay, the effect remained negative, reaching a value around 0% after 4 h.

Méndez-Arriaga et al. [56] investigated the efficiency of TiO_2-photocatalytic treatment in degrading three non-steroidal anti-inflammatory drugs (NSAIDs) (i.e. ibuprofen, diclofenac and naproxen) under varying conditions of temperature, TiO_2 loading and dissolved-oxygen concentration. Several hydroxylated derivatives of ibuprofen were identified as primary degradation products, to be followed by demethylation and decarboxylation. The increase in inhibition of bioluminescence was observed in the first 120 min and 240 min in the solution with excess and lack of oxygen, respectively, due to the formation of toxic by-products. Interestingly, the authors reported that the intensity of by-products in the non-saturated conditions was double that observed for the oxygen-saturated solution.

Li et al. [60] observed formation of more toxic initial intermediates of ozonation of oxytetracycline, with an inhibitory effect on bioluminescence of *V. fischeri* increasing up to 99.5% after the first 60 min at pH 3, with a dramatic decrease to 32% in the next 60 min. Under neutral and basic conditions (i.e. pH 7 and 11), the evolution of toxicity was similar but with a faster decay from the maximum value.

Pérez-Estrada et al. [50] observed higher toxicity on *V. fischeri* when treating dipyrone by TiO_2-assisted photocatalysis than by photo-Fenton photocatalysis, although the same intermediate products were formed. This was due to the fact that, in TiO_2 photocatalysis, the amount of 4-methylaminoantipiryne (MAA), the hydrolytic product of dipyrone, was higher, and, when only MAA was present at t = 0, toxicity was already at the 50% threshold. The toxicity determined for photo-Fenton treatment was always below the 50% bioluminescent bacteria-inhibition threshold, whereas, in the TiO_2-photocatalytic treatment, it was found to be higher. Attention should therefore be paid when discharging MAA into the environment.

Similar to previously mentioned studies, in TiO_2-photocatalytic treatment of salbutamol, the highest toxicity observed (i.e. 54%) coincided with the highest amount of degradation products measured [54]. Considering that the toxicity of the initial solution of salbutamol was only 4%, attention should be paid when optimizing the TiO_2-photocatalytic treatment since more hazardous products are formed. Fig. 5 shows the evolution of toxicity along the TiO_2-photocatalytic degradation of salbutamol.

Besides the *V. fischeri* bioluminescence assay, a short-term 4–24 h *D. magna* feeding-response assay is also applied for determination of acute toxicity. It is based on algae-clearance rates, since feeding in *D. magna* and many other aquatic organisms is physiologically linked with growth and reproduction, hence effects on feeding are usually translated to population responses [61].

Beltrán et al. [62] compared the efficiencies and toxicity evolution of the aqueous solution of sulfamethox-

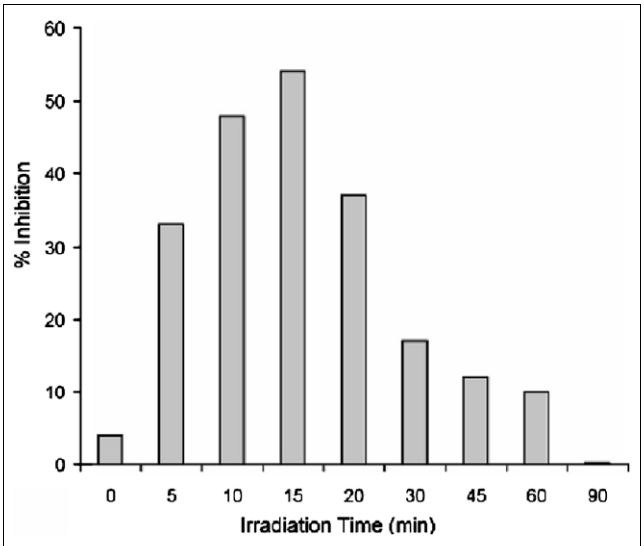

Figure 5. Inhibition (%) of the luminescence of bacteria *Vibrio fischeri* as a function of photocatalytic treatment time (reproduced from [55] with permission of Elsevier).

azole treated by UVA radiation, ozonation, catalytic ozonation (O_3/TiO_2), ozone photolysis (O_3/UVA), photocatalytic ozonation (O_3/TiO_2/UVA) and photocatalytic oxidation (O_2/TiO_2/UVA). Acute-toxicity *D. magna* assays were conducted using the commercial test kit Daphtoxkit F, in accordance with OECD guideline 202 (Daphnia sp. Acute Immobilization Test) [63]. The results indicated that oxidation of sulfamethoxazole led to intermediates that still exhibited some sort of toxicity [62]. The toxicities observed at the end of the experiments were most probably due to unknown intermediates, since the effect of the detected concentrations of carboxylic acids (oxalic, maleic and fumaric acid) were below the observed EC_{50} value.

However, these short-term acute-toxicity assays are not always adequate indicators of toxicity. For example, the Microtox test, developed in the 1980s, is primarily testing lethality (like many other currently applied bioassays) (i.e. acute toxicity rather than chronic toxicity). With the development of highly sensitive, selective analytical equipment measuring ng/L and pg/L concentrations of contaminants, the assessment of long-term toxicity, potentially causing subtle ecotoxicological effects, seems more relevant than predicting acute toxicities at the mg/L level. The extrapolation of laboratory-based determinations of lethal concentrations (LCs) to the effects of pharmaceuticals at environmentally-relevant ng/L levels is uncertain, whereas subtle effects, other than threshold toxicity, would be expected for environmentally-relevant concentrations of pharmaceuticals [64]. More importantly, potential modes of action (MOAs) of pharmaceuticals on non-target aquatic organisms could differ significantly from the MOAs investigated when conducting tests, such as Microtox and other acute-toxicity tests. As observed by Sanderson and Thomsen [65], the approach applied so far by the scientific community can be described by the ''lamppost analogy'' – ''Looking for the car keys under the street lamppost – even though they got lost by the building's front door in the dark''.

Furthermore, Seiler [66] pointed out that even slight, non-significant influences on single components within regulatory cascades (e.g., cellular division or signal transduction), which would not result in any acute effect, might ultimately adversely affect the entire population through sequential propagation or interactions with additional, unrelated factors. Acute-toxicity bioassays conducted on a few selected eco-organisms could be insufficient to predict the hazardousness of a compound, especially in the case of pharmaceuticals, the potential effects of which may not be detected by such tests. Seiler et al. [66] proposed consideration of pharmacodynamic properties of drugs, necessary effect concentrations and range of activities in order to derive a potential ecotoxicological profile.

There has been some assessment of adverse effects related to sub-lethal effects (e.g., mutagenic effects, alterations in immune and endocrine systems, genotoxic effects and reproduction-rate decline [67,68]) performed with secondary wastewater effluent. For example, Petala et al. [69] used the Ames test together with the Microtox assay to estimate the mutagenicity of secondary wastewater effluent treated with ozone. The Ames assay is a bacterial reverse-mutation assay that evaluates the genotoxicity of a compound by measuring its ability to induce reverse mutations at selected loci in a bacterial strain. Usually, the compensating mutation must occur by the same mutagenic mechanism, so mechanistic toxicology information is available from Ames-assay results based on the pattern of which strain reverted. It was found that ozonation at mild conditions (i.e. low O_3 doses and short ozonation times) augmented mutagenicity, possibly due to the formation of intermediate TPs, whereas, by intensifying the ozonation conditions, these compounds were further degraded to non-mutagenic products.

Nakamura et al. [70] investigated mutagenic effects of chlorination products of two nitrofuran antibiotics (nitrofurazone and frazolidone) by Ames assay [i.e. exposure to *Salmonella typhimurium* strain TA100 without rat-liver homogenate (S9 mix)]. The *S. typhimurium* strain used in the assay has a unique mutation that has turned off histidine biosynthesis in the bacteria, which can then undergo a reverse mutation turning the essential gene back on to permit the cell to grow in the absence of either histidine or tryptophan (prototrophy). The bacteria use the trace histidine or tryptophan to undergo several cell divisions, but will stop growing once they have run out, leaving a characteristic ''background lawn'' that decreases in density with increasing toxicity. After 48 h, only those cells that have undergone a reverse mutation turning the essential gene back on have survived, producing mutant colonies. The background lawn density is scored and the number of revertant colonies then counted. Mutation results are reported as revertants per plate. For the chlorinated solution of frazolidone, Nakamura et al. [70] recorded no mutagenic response, whereas chlorination by-products of nitrofurazone [i.e. 5-nitro-2-furaldehyde (NFA), 5-nitro-2-furoic acid (NFOA), 5-hydroxy-2-furoic acid (HFA), 5-hydroxymethylene-2-(5H)-furanone (HMF), and chlorinated product of nitrofurazone] exhibited mutagenic effects on the TA100 strain without the S9 mix.

Short-term, sub-lethal, toxicity assays are frequently applied to predict long-term ecological effects of toxic compounds [71]. Palominos et al. [72] investigated the susceptibility of *Escherichia coli* strains inoculated at agar plates to inhibition by reaction products of TiO_2-photocatalytic degradation antibiotic flumequine. A clear correlation between depletion of antibiotic and total antibacterial activity was found, since the inhibition halo around the microdrop seeded at the agar plate disappeared completely for samples after 30 min of irradia-

tion, the time that was necessary for complete elimination of flumequine.

Andreozzi et al. [73] reported ozonation to be an efficient technique for reducing the toxicity of antibacterial agent lincomycin. An Agar diffusion test and liquid growth-inhibition tests against lincomycin performed with different microalgal strains revealed EC_{50} values varying from 195 μg/L for *S. leopoliensis* to 1.51 mg/L for *P. subcapitata* and 1.63 mg/L for *C. meneghiniana*, whereas the resulting ozonation samples were less toxic after only 1 h of treatment.

Baran et al. [74] investigated the toxicity of sulfonamides (sulfacetamide, sulfamethoxazole, sulfadiazine and sulfathiazole) and their TiO_2-photocatalytic degradation products in experiments with green alga *Chlorella vulgaris*. Their growth was monitored by measuring spectrophotometrically at 680 nm the optical density of the cell suspension with the added treated sample after 48 h absorbance, and comparing it to the control sample. It was found that all four sulfonamides were toxic to *C. vulgaris*, whereas photocatalytic degradation products were estimated to be less toxic than the original drugs.

Andreozzi et al. [75] performed toxicity tests by exposing algae (*S. leopoliensis*) and invertebrates (*Brachionus calyciflorus*-rotifer) to aqueous samples containing the mixture of six pharmaceuticals (i.e. carbamazepine, clofibric acid, diclofenac, sulfamethoxazole, ofloxacin and propranolol) treated for different reaction times by oxidative techniques (i.e. ozonation, H_2O_2/UV and TiO_2 photocatalysis). Ozonation and UV/H_2O_2 reduced the toxicity on rotifers after 2 min and 3 min, respectively, whereas for algae this time was even shorter (1 min). Moreover, after 3–5 min, the growth of algae was stimulated, possibly due to the usage of intermediates formed as a carbon source. However, TiO_2-photocatalytic treatment displayed the formation of toxic intermediates, since, even after 48 h, the inhibition effect on algae and invertebrates was observed to be 69–83% and 75–85%, respectively.

Since pharmaceuticals and their degradation products may affect organisms from different trophic levels, toxicity should be evaluated by a battery of different bioassays, since the intermediates formed will exhibit different toxicities, depending on the test applied. For example, bioassays with *V. fischeri*, *D. magna* and *Microalga* measured different changes in the toxicity of the solution of pesticides during photo-Fenton photocatalysis and TiO_2 photocatalysis, for the same levels of TOC [76].

High-throughput assays that use cells or cell lines, preferably of human origin, to evaluate the toxicities of compounds may measure relatively simple processes (e.g., binding of environmental agent with cellular protein and changes in gene expression caused by that binding) or more integrated responses (e.g., cell division and cell differentiation). Yargeau et al. [77] used human primary liver cancer cells HepG2 for the determination of toxicity of sulfamethoxazole and its ozonation products, due to their long proliferation time. The ozonation products of sulfamethoxazole, including sulfanilamide (active agent of Prontosil and the first sulfa drug discovered), methanol, ethanol and phenol, stimulated proliferation of HepG2 and an increase in cell metabolism, instead of deteriorating it. But, it was impossible to distinguish which degradate was provoking those changes or which cell functions were affected by the morphological changes observed.

However, Bedner et al. [18] reported two toxic degradation products of acetaminophen as a result of treatment with hypochlorite, NAPQI and 1,4-benzoquinone. NAPQI is a toxic metabolite of acetaminophen formed in liver at higher administered doses [78], provoking hepatic necrosis. This compound readily hydrolyzes in aqueous solution to 1,4-benzoquinone [79], a benzene metabolite implicated in genotoxic and mutagenic effects [80]. As regards the evolution profiles of the toxic products of acetaminophen chlorination, NAPQI reached its maximum concentration after 10 min, and then decayed to form 1,4-benzoquinone. The concentration of 1,4-benzoquinone increased over time to ~25% of the initial concentration of acetaminophen after 1 h of chlorination, while, at that time for NAPQI, it was only 1.5%. In the study where acetaminophen, NAPQI and 1,4-benzoquione were intraperitoneally injected into mouse, their LD50 toxicities were 500 mg/kg, 20 mg/kg and 8.5 mg/kg, respectively [79]. In other words, NAPQI and 1,4-benzoquinone were 25 times and 58 times more toxic than acetaminophen itself. NAPQI and 1,4-benzoquinone are not likely to persist in wastewater treatment where sulfite is employed during dechlorination, since they would probably be reduced into acetaminophen and 1,4-hydroquinone, respectively.

In their study on the UV/H_2O_2 oxidation of carbamazepine, Vogna et al. [81] reported acridine intermediates as the main products of the radical-degradation pathway, which are more toxic than the parent compound due to their mutagenic and carcinogenic activity [82], so failure to ensure complete mineralization of carbamazepine in UV/H_2O_2 treatment may worsen environmental and health impacts of water contamination by carbamazepine.

The change in toxicity during processes such as chlorination, ozonation and AOPs will depend on the mechanism of reaction of a certain compound (i.e. whether the moieties essential to the activity of the molecule react or not). For example, Lange et al. [83] reported that ozonation of macrolide antibiotics, namely clarithromycin, leading to N-oxidation of the dimethylamino group inactivates these drugs, as assayed by suppression of the growth of *Pseudomonas putida*. The macrolide antibiotics are thought to block the tunnel that channels the nascent peptides away from the pep-

Table 2. Antibacterial substrates and expected sites of O_3 attack. Adapted from Dodd et al. [87].

Macrolides

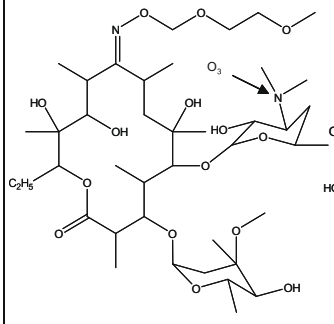

Roxithromycin
pKa=9.2

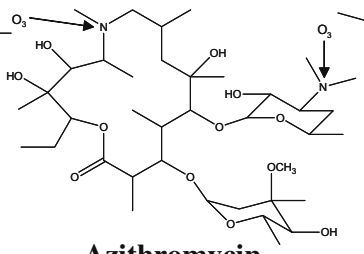

Azithromycin
pKa $_{1,2}$=8.7, 9.5

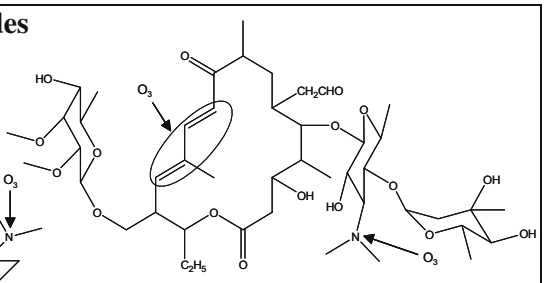

Tylosin
pKa=7.7

Sulfonamides

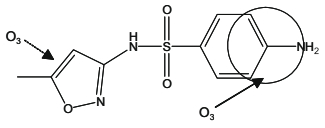

Sulfamethoxazole
pKa $_{1,2}$=1.7, 5.6

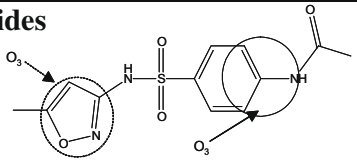

N(4)-acetyl-sulfamethoxazole
pKa=5.5

DHFR[a] Inhibitor

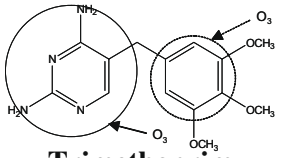

Trimethoprim
pKa $_{1,2}$=3.2, 7.1

Fluoroquinolones

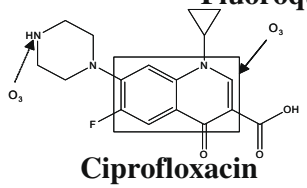

Ciprofloxacin
pKa $_{1,2}$=6.2, 8.8

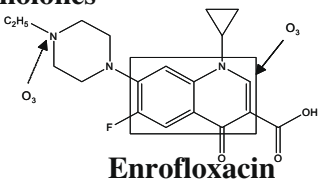

Enrofloxacin
pKa $_{1,2}$=6.1, 7.7

Lincosamide

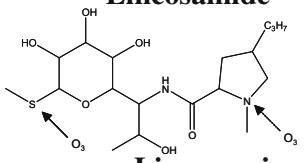

Lincomycin
pKa=7.8

ß-lactams

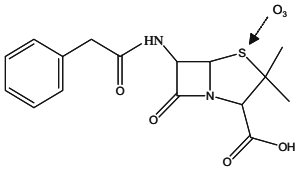

Penicilin G
pKa=2.7

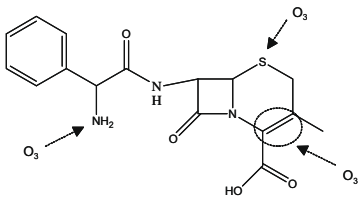

Cephalexin
pKa $_{1,2}$=2.5, 7.1

Tetracycline

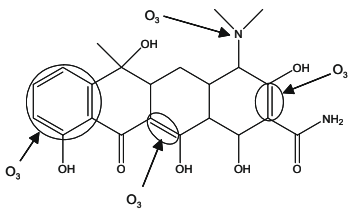

Tetracycline
pKa $_{1,2,3}$=3.3, 7.7, 9.7

Aminoglycoside

Amikacin
pKa $_{1,2,3,4}$=6.7, 8.4, 8.4, 9.7

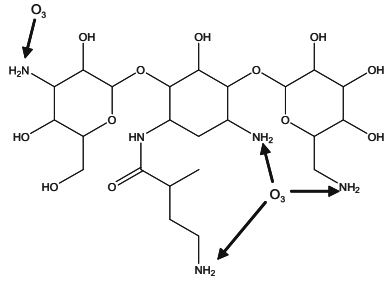

[a]DHFR, dihydrofolate reductase.

tidyl-transferase center inside the ribosome. For this function, the dimethylamino group of the desosamine sugar is considered the major domain necessary for binding the macrolide to its target [84], so N-oxidation of macrolides would deactivate them as ribosomal antibiotics. Acetalization of the keto group of clarithromycin was also noted during ozonation, which was also considered to lower the biological activity [84].

Dodd and Huang [85] reported that, during chlorination of trimethoprim, halogenation and/or oxidation reactions took place at the 2,4-diaminopyrimidinyl moiety, leading to the formation of (multi)chlorinated and hydroxylated products. Since the antibacterial activity of trimethoprim is derived from its 2,4-diamino-5-methylpyrimidine moiety, which blocks bacterial folate synthesis by occupying available dihydrofolate reductase enzymes [86], and this group is extensively substituted in reactions with free chlorine, it is likely that chlorination will reduce the antibacterial activity.

As argued by Dodd et al. [87], some antibiotics may react in ozonation preferentially with moieties not essential to the biochemical activities of the parent molecule, or they can simply be refractory to O_3. For example, the flumequine moiety in fluoroquinolone antibiotics ciprofloxacin and enrofloxacin (see Table 2) will react with O_3 14 times and 109 times slower, respectively, at pH 7 than their non-essential piperazine moiety, so, in these cases, loss of an original drug does not necessarily correspond to loss of antibacterial activity. Also, essential functional groups of N_4-acetyl-sulfamethoxazole and ß-lactams are possibly not sufficiently oxidized during ozonation. For ß-lactam penicillin G, reaction with the $^{\bullet}OH$ radical will be more desirable than oxidation by O_3, since it will result in biochemically-inactive products benzylpenilloic acid and benzylpenicilloic acid. Similarly, O_3 appears to react only very slowly with the biochemically essential *p*-sulfonylaniline group in N_4-acetyl-sulfamethoxazole. However, amikacin should preferentially be degraded by O_3, considering that the $^{\bullet}OH$ radical attack occurs at sites not associated with the antibacterial activity of the molecule.

Another approach to evaluating the toxicity of pharmaceuticals and their degradation products is through modeling programs (e.g., ECOSAR). ECOSAR predicts the toxicity of compounds to aquatic organisms (e.g., fish, invertebrates and algae) by using (Quantitative) Structure Activity Relationships [(Q)SARs]. The program estimates an acute (short-term) toxicity and, when available, chronic (long-term or delayed) toxicity. The assessment program uses a number of log Kow-based (Q)SARs to estimate the ecotoxicity of organic compounds for several structural classes, often resulting in ecotoxicity estimates of a variety of endpoints. For example, the (Q)SAR model was found to underestimate the acute toxicity (24 h to 21 days) of pharmaceuticals, relative to the data measured in standardized tests [88]. ECOSAR can be downloaded freely from the US EPA website (http://www.epa.gov/oppt/exposure/docs/episuitedl.htm).

Buth et al. [29] used ECOSAR to determine the predicted no-effect concentration (PNEC) of cimetidine and its chlorination products. From the toxicity predicted by ECOSAR, intermediates 4-hydroxymethyl-5-methyl-1H-imidazole and 4-chloro-5-methyl-1H-imidazole were estimated to be more toxic than cimetidine itself, whereas 4-chloro-5-methyl-1H-imidazole had a PNEC derived from LC_{50} of 6.5 μg/L, the same order of magnitude as for atrazine and 2,4-dichlorophenol [29]. However, PNECs calculated for cimetidine sulfoxide and both ß-sultam and δ-sultam (based on EC_{50}) were relatively high (of the order of 100 μg/L). Moreover, the experiments performed with NH_4Cl as quenching agent of free chlorine demonstrated that the same TPs are likely to be formed even during wastewater treatment.

The intermediates formed during drinking-water and wastewater treatment deserve special attention, even when their measured toxicities and biological activities are of minor importance. For example, an N-chlorinated intermediate identified as a product of chlorination of sulfamethoxazole was observed to decay by ring chlorination or back reaction to the parent compound [30]. Considering that dechlorination is a common practice in most WWTPs, this could lead to release of sulfamethoxazole from its N-chlorinated product.

6. Conclusions and future trends

Even though disappearance of the original drug is easily achieved in chlorination, ozonation and AOPs, by-products generated can be less biodegradable and/or more toxic than the parent compound. The complex nature of photolytic transformations and oxidative/reductive reactions taking place in such processes underscores the need to elucidate structures and potentially additive, antagonistic and synergetic ecotoxicological effects of intermediate TPs. The environmental hazard of pharmaceuticals may be enhanced via association with complex mixtures of other pharmaceuticals, their human metabolites and degradation products, as well as other residues present in municipal wastewater.

Despite difficulties in understanding the effects that chronic exposure to pharmaceutical residues have on human and environmental health, existing studies show that their input into the environment must be controlled and reduced as far as possible. Regulatory and risk management relating to pharmaceutical residues in the environment is complex, taking into account their low acute risks, uncertain bioavailability and MOAs on non-target organisms, potentially additive effects in the presence of degradation products, intrinsic toxicity and bacterial resistance. Ultimately, those challenges should

be faced with case-by-case studies. As information on exposure to and biological effects of pharmaceuticals increases, estimations of the safety margin between the no-effect concentration and expected exposure concentration in water will be more precise, and hazard assessment of any particular drug will become more reliable.

Acknowledgments

The work was financially supported by the Spanish Ministry of Science and Innovation, projects SOSTAQUA (led by Aguas de Barcelona and founded by CDTI in the framework of the Ingenio 2010 Programme under the CENIT call) and CEMAGUA (CGL2007-64551/HID), and the Unity Through Knowledge Fund (UKF), which was established by the Croatian Ministry of Science, Education and Sports through the World Bank Loan No. 7320-HR. J.R. gratefully acknowledges the JAE Program (Junta para la Ampliación de los Estudios), co-financed by CSIC (Consejo Superior de Investigaciones Científicas) and European Social Funds, for a predoctoral grant.

References

[1] R.B. Silverman (Editor), The Organic Chemistry of Drug Design and Drug Action, Academic Press, San Diego, CA, USA, 1992.
[2] J. Radjenović, M. Petrović, D. Barceló, Trends Anal. Chem. 26 (2007) 1132.
[3] J.P. Sumpter, Toxicol. Lett. 102–103 (1998) 337.
[4] K. Kummerer, J. Antimicrob. Chemother. 54 (2004) 311.
[5] B. Halling-Sørensen, S.N. Nielsen, P.F. Lanzky, F. Ingerslev, H.C.H. Lützhøft, S.E. Jørgensen, Chemosphere 36 (1998) 357.
[6] C.G. Daughton, T.A. Ternes, Environ. Health Perspect. 107 (1999) 907.
[7] D.B. Huggett, B.W. Brooks, B. Peterson, C.M. Foran, D. Schlenk, Arch. Environ. Contam. Toxicol. 43 (2002) 229.
[8] A. Villegas-Navarro, L.E. Rosas, J.L. Reyes, Comp. Biochem. Physiol., C: Toxicol. Pharmacol. Endocrinol 136 (2003) 127.
[9] M. Cleuvers, Chemosphere 59 (2005) 199.
[10] B.I. Escher, N. Bramaz, M. Richter, J. Lienert, Environ. Sci. Technol. 40 (2006) 7402.
[11] N. Laville, S. Ait-Assa, E. Gomez, C. Casellas, J.M. Porcher, Toxicology 196 (2004) 41.
[12] E.A. Tendencia, L.D. De La Pena, Aquaculture 195 (2001) 193.
[13] C. Mimeault, A.J. Woodhouse, X.S. Miao, C.D. Metcalfe, T.W. Moon, V.L. Trudeau, Aquat. Toxicol. 73 (2005) 44.
[14] K. Ikehata, N.J. Naghashkar, M.G. El-Din, Ozone Sci. Eng. 28 (2006) 353.
[15] O. Legrini, E. Oliveros, A.M. Braun, Chem. Rev. 93 (1993) 671.
[16] T. Oppenlander (Editor), Photochemical Purification of Water and Air: Advanced Oxidation Processes (AOPs): Principles, Reaction Mechanisms, Reactor Concepts, Wiley-VCH Verlag, Weinheim, Germany, 2003.
[17] F.J. Beltrán (Editor), Ozone Reaction Kinetics for Water and Wastewater Systems, Lewis Publishers, Boca Ratón, FL, USA, 2003.
[18] M. Bedner, W.A. MacCrehan, Environ. Sci. Technol. 40 (2006) 516.
[19] R. Rosal, A. Rodríguez, J.A. Perdigón-Melón, A. Petre, E. Garcóa-Calvo, M.J. Gómez, A. Agüera, A.R. Fernández-Alba, Chemosphere 74 (2009) 825.
[20] E. Evgenidou, I. Konstantinou, K. Fytianos, T. Albanis, J. Hazard. Mater., B 137 (2006) 1056.
[21] C. Sirtori, A. Zapata, I. Oller, W. Gernjak, A. Agüera, S. Malato, Water Res. 43 (2009) 661.
[22] T. Kosjek, E. Heath, Trends Anal. Chem. 27 (2008) 807.
[23] T. Kosjek, E. Heath, M. Petrović, D. Barceló, Trends Anal. Chem. 26 (2007) 1076.
[24] X. Zhang, F. Wu, X. Wei Wu, P. Chen, N. Deng, J. Hazard. Mat. 157 (2008) 300.
[25] R. Andreozzi, V. Caprio, R. Marotta, D. Vogna, Water Res. 37 (2003) 993.
[26] D.A. Lambropoulou, M.D. Hernando, I.K. Konstantinou, E.M. Thurman, I. Ferrer, T.A. Albanis, A.R. Fernández-Alba, J. Chromatogr., A 1183 (2008) 38.
[27] L.A. Pérez-Estrada, S. Malato, W. Gernjak, A. Agüera, E.M. Thurman, I. Ferrer, A.R. Fernández-Alba, Environ. Sci. Technol. 39 (2005) 8300.
[28] D.C. McDowell, M.M. Huber, M. Wagner, U. Von Gunten, T.A. Ternes, Enivron. Sci. Technol. 39 (2005) 8014.
[29] J.M. Buth, W.A. Arnold, K. McNeill, Environ. Sci. Technol. 41 (2007) 6228.
[30] M.C. Dodd, C.H. Huang, Environ. Sci. Technol. 38 (2004) 5607.
[31] T.E. Doll, F.H. Frimmel, Water Res. 38 (2004) 955.
[32] T.E. Doll, F.H. Frimmel, Catal. Today 101 (2005) 195.
[33] M. Bedner, W.A. MacCrehan, G.R. Helz, J. Chromatogr. Sci. 40 (2002) 447.
[34] S. Pérez, P. Eichhorn, M.D. Celiz, D.S. Aga, Anal. Chem. 78 (2006) 1866.
[35] P. Eichhorn, P.L. Ferguson, S. Pérez, D.S. Aga, Anal. Chem. 77 (2005) 4176.
[36] G. Hopfgartner, E. Varesio, V. Tschappat, C. Grivet, E. Bourgogne, L.A. Leuthold, J. Mass Spectrom. 39 (2004) 845.
[37] T. Paul, P.L. Miller, T.J. Strathmann, Environ. Sci. Technol. 41 (2007) 4720.
[38] B. De Witte, J. Dewulf, K. Demeestere, V. Van De Vyvere, P. De Wispelaere, H. Van Langenhove, Environ. Sci. Technol. 42 (2008) 4889.
[39] P. Calza, M. Pazzi, C. Medana, C. Baiocchi, E. Pelizzetti, J. Pharm. Biomed. Anal. 35 (2004) 9.
[40] P. Calza, V.A. Sakkas, C. Medana, C. Baiocchi, A. Dimou, E. Pelizzetti, T. Albanis, Appl. Catal., B 67 (2006) 197.
[41] H.G. Wetzstein, N. Schmeer, W. Karl, Appl. Environ. Microbiol. 63 (1997) 4272.
[42] S. Bielecka-Grzela, A. Klimowicz, J. Clin. Pharm. Therap. 30 (2005) 383.
[43] D.T.W. Chu, P.B. Fernandes, Antimicrob. Agents Chemother. 33 (1989) 131.
[44] H.J. Zeiler, U. Petersen, W. Gau, H.J. Ploschke, Arzneimittel-Forschung/Drug Res. 37 (1987) 131.
[45] P. Calza, C. Medana, M. Pazzi, C. Baiocchi, E. Pelizzetti, Appl. Catal., B 53 (2004) 63.
[46] I. Dalmázio, M.O. Almeida, R. Augusti, T.M.A. Alves, J. Am. Soc. Mass Spectrom. 18 (2007) 679.
[47] J.M. Campbell, B.A. Collings, D.J. Douglas, Rapid Comm. Mass Spectrom. 12 (1998) 1463.
[48] J. Radjenović, C. Sirtori, M. Petrović, D. Barceló, S. Malato, Environ. Sci. Technol. (2009), submitted for publication.
[49] J. Radjenović, C. Sirtori, M. Petrović, D. Barceló, S. Malato, Appl. Catal. B. (2009), in press, doi:10.1016/j.apcatb.2009.02.013.
[50] L.A. Pérez-Estrada, S. Malato, A. Agüera, A.R. Fernández-Alba, Catal. Today 129 (2007) 207.
[51] A.G. Marshall, C.L. Hendrickson, G.S. Jackson, Mass Spectrom. Rev. 17 (1998) 1.
[52] A. Makarov, E. Denisov, A. Kholomeev, W. Balschun, O. Lange, K. Strupat, S. Horning, Anal. Chem. 78 (2006) 2113.
[53] C. Medana, P. Calza, F. Carbone, E. Pelizzeti, H. Hidaka, C. Baiocchi, Rapid Comm. Mass Spectrom. 22 (2008) 301.

[54] V.A. Sakkas, P. Calza, C. Medana, A.E. Villioti, C. Baiocchi, E. Pelizzetti, T. Albanis, Appl. Catal., B 77 (2007) 135.
[55] R.F. Dantas, M. Canterino, R. Marotta, C. Sans, S. Esplugas, R. Andreozzi, Water Res. 41 (2007) 2525.
[56] F. Méndez-Arriaga, S. Esplugas, J. Giménez, Water Res. 42 (2008) 585.
[57] P. Calza, V.A. Sakkas, A. Villioti, C. Massolino, V. Boti, E. Pelizzetti, T. Albanis, Appl. Catal., B 84 (2008) 379.
[58] R.F. Dantas, S. Contreras, C. Sans, S. Esplugas, J. Hazard. Mater. 150 (2008) 790.
[59] R. Grande, S. Di Pietro, E. Di Campli, S. Di Bartolomeo, B. Filareto, L. Cellini, J. Environ. Sci. Health, Part A 42 (2007) 33.
[60] K. Li, A. Yediler, M. Yang, S. Schulte-Hostede, M.H. Wong, Chemosphere 72 (2008) 473.
[61] C. Barata, D.J. Baird, Aquat. Toxicol. 48 (2000) 195.
[62] F.J. Beltrán, A. Aguinaco, J.F. García-Araya, A. Oropesa, Water Res. 42 (2008) 3799.
[63] Organization for Economic Cooperation and Development (OECD), OECD Guidelines for the Testing of Chemicals, Section 2: Effects on Biotic Systems, Test No. 202: Daphnia sp. Acute Immobilisation Test, OECD Publishing, Paris, France, 2004.
[64] E.J. Calabrese, J.W. Staudenmayer, E.J. Stanek, G.R. Hoffmann, Toxicol. Sci. 94 (2006) 368.
[65] H. Sanderson, M. Thomsen, Bull. Environ. Contam. Toxicol. 79 (2007) 331.
[66] J.P. Seiler, Toxicol. Lett. 131 (2002) 105.
[67] S. Aguayo, M.J. Muñoz, A. De La Torre, J. Roset, E. De La Peña, M. Carballo, Sci. Total Environ. 328 (2004) 69.
[68] H. Dizer, E. Wittekindt, B. Fischer, P.D. Hansen, Chemosphere 46 (2002) 225.
[69] M. Petala, P. Samaras, A. Zouboulis, A. Kungolos, G.P. Sakellaropoulos, Water Res. 42 (2008) 4929.
[70] H. Nakamura, T. Kawakami, T. Niino, Y. Takahashi, S. Onodera, J. Toxicol. Sci. 33 (2008) 621.
[71] C. Barata, P. Alanon, S. Gutierrez-Alonso, M.C. Riva, C. Fernández, J.V. Tarazona, Sci. Total Environ. 405 (2008) 78.
[72] R. Palominos, J. Freer, M.A. Mondaca, H.D. Mansilla, J. Photochem. Photobiol., A 193 (2008) 139.
[73] R. Andreozzi, M. Canterino, R.L. Giudice, R. Marotta, G. Pinto, A. Pollio, Water Res. 40 (2006) 630.
[74] W. Baran, J. Sochacka, W. Wardas, Chemosphere 65 (2006) 1295.
[75] R. Andreozzi, L. Campanella, B. Fraysse, J. Garric, A. Gonnella, R. Lo Giudice, R. Marotta, G. Pinto, A. Pollio, Water Sci. Technol. 50 (2004) 23.
[76] A.R. Fernández-Alba, D. Hernando, A. Agüera, J. Cáceres, S. Malato, Water Res. 36 (2002) 4255.
[77] V. Yargeau, J.C. Huot, A. Rodayan, L. Rouleau, R. Roy, R.L. Leask, Environ. Toxicol. 23 (2008) 492.
[78] J.G.M. Bessems, N.P.E. Vermeulen, Crit. Rev. Toxicol. 31 (2001) 55.
[79] D.C. Dahlin, S.D. Nelson, J. Med. Chem. 25 (1982) 885.
[80] R. Snyder, J. Toxicol Environ. Health. Part A 61 (2000) 339.
[81] D. Vogna, R. Marotta, R. Andreozzi, A. Napolitano, M. d'Ischia, Water Res. 54 (2004) 497.
[82] S.M. Furst, J.P. Uetrecht, Biochem. Pharmacol. 45 (1993) 1267.
[83] F. Lange, S. Cornelissen, D. Kubac, M.M. Sein, J. von Sonntag, C.B. Hannich, A. Golloch, H.J. Heipieper, M. Möder, C. von Sonntag, Chemosphere 65 (2006) 17.
[84] F. Schlünzen, R. Zarivach, J. Harms, A. Bashan, A. Tocilj, R. Albrecht, A. Yonath, F. Franceschi, Nature (London) 413 (2001) 814.
[85] M.C. Dodd, C.H. Huang, Water Res. 41 (2007) 647.
[86] C. Walsh (Editor), Antibiotics: Actions, Origins, Resistance, ASM Press, Washington DC, USA, 2003.
[87] M.C. Dodd, M.-O. Buffle, U. von Gunten, Environ. Sci. Technol. 40 (2006) 1969.
[88] H. Sanderson, D.J. Johnson, C.J. Wilson, R.A. Brain, K.R. Solomon, Toxicol. Lett. 144 (2003) 383.